

ChemComm

Accepted Manuscript



This is an *Accepted Manuscript*, which has been through the Royal Society of Chemistry peer review process and has been accepted for publication.

Accepted Manuscripts are published online shortly after acceptance, before technical editing, formatting and proof reading. Using this free service, authors can make their results available to the community, in citable form, before we publish the edited article. We will replace this *Accepted Manuscript* with the edited and formatted *Advance Article* as soon as it is available.

You can find more information about *Accepted Manuscripts* in the [Information for Authors](#).

Please note that technical editing may introduce minor changes to the text and/or graphics, which may alter content. The journal's standard [Terms & Conditions](#) and the [Ethical guidelines](#) still apply. In no event shall the Royal Society of Chemistry be held responsible for any errors or omissions in this *Accepted Manuscript* or any consequences arising from the use of any information it contains.

Cite this: DOI: 10.1039/c0xx00000x

www.rsc.org/xxxxxx

ARTICLE TYPE

Integration of Graphene Oxide and DNA as Universal Platform for Multiple Arithmetic Logic Units

Kun Wang,^{a,b} Jiangtao Ren,^a Daoqing Fan,^a Yaqing Liu,^{*a} and Erkang Wang^{*a}

Received (in XXX, XXX) Xth XXXXXXXXX 20XX, Accepted Xth XXXXXXXXX 20XX

DOI: 10.1039/b000000x

By combination of graphene oxide with DNA, a universal platform was developed for integration of multiple logic gates to implement both half adder and half subtractor functions. A constant undefined threshold range between high and low fluorescence output signals was set for all the developed logic gates.

Untraditional molecular computing is scientifically interesting and presents potential applications in extensive research fields.^{1,2} A key requirement of data processing is the ability to combine multiple molecular logic gates to perform arithmetic functions.^{3,4} Chemical logic gates are already able to perform basic and complex functions.⁵⁻⁸ As a powerful medium of processing information, DNA with well-ordered and predictable structure has been considered as excellent candidate for engineering of biomolecular circuits.⁹⁻¹³ Aptamer opens a new avenue for the design of biomolecular devices and logic gates due to its high specificity and affinity with extensive targets.^{14, 15} Large efforts have been focused on the fabrication of DNA-based logic gates with Boolean functions.¹⁶⁻²¹ With significant development of nanomaterials, the combination of biomolecules and nanomaterials has attracted great attention in various research fields such as nanotechnology, biosensors, molecular devices and materials science.²²⁻²⁶ Water-soluble nanomaterial, graphene oxide (GO), has been demonstrated to be promising platform for the construction of bioelectronic devices and biosensors due to the unique electronic, optical, mechanical and catalytic properties.^{27, 28} Various of logic gates performing basic Boolean functions have been developed on the basis of the combination of GO and DNA (GO/DNA).^{27, 29-33} To fulfill the requirements of increased computational complexity, however, it is of importance to integrate multiple and combinatorial logic gates in a universal platform, which is rarely reported.³⁴⁻³⁶ Encouraged by the progress on molecular logic gates, herein, multiple logic gates were integrated on a universal GO/DNA platform for the first time to implement both arithmetic functions of half adder (HA) and half subtractor (HS).

A half adder is in high demand in information technology and can be used to construct more advanced computational circuits.¹⁷ It can perform an addition operation of two binary digits by integration of an XOR gate and an AND gate in parallel to generate a SUM (S) output and a CARRY (C) output, respectively. And a half subtractor can perform a subtraction of two bits, which requires the combination of an XOR gate and an

INHIBIT gate to produce a DIFFERENCE (D) output and a BORROW (B) output, respectively. The implementation of all logic gates is based on output signal switching between “1” and “0” triggered by inputs. Herein, two distinct fluorescent dyes FAM (6-carboxyfluorescein) and NMM (N-methylmesoporphyrin IX) were selected as signal reporter for the required logic gates of HA and HS.

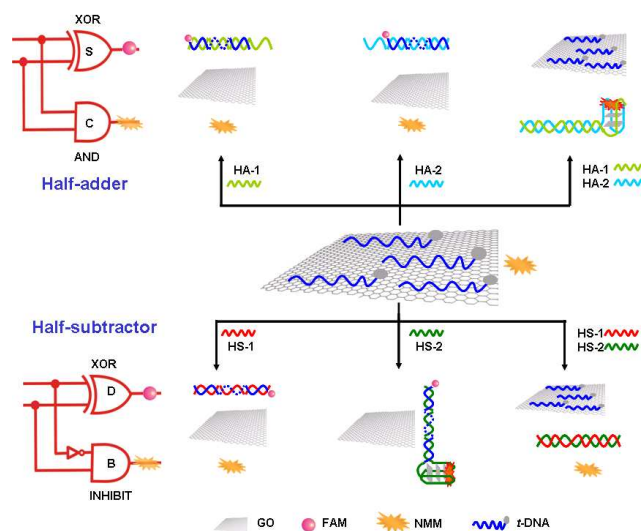


Fig. 1 The operation mechanism of the developed half adder and half subtractor with the corresponding circuits.

Fig. 1 outlines the operation mechanism. FAM labelled ss-DNA was used as the template DNA (*t*-DNA) and mixed with GO and NMM as the initial platform. The fluorescent signal of NMM can be significantly enhanced once binding on G-quadruplex (G-4),^{37, 38} whose formation depends on the interaction among the designed inputs and the platform. It is interesting that GO can act as a super nanoquencher to quench the fluorescence of various dyes via long-range resonance energy transfer (LrRET)³⁹ and can also differentiate DNA structures such as single-stranded DNA (ss-DNA), double-stranded DNA (ds-DNA) and G-quadruplex.⁴⁰ ss-DNA can be trapped on GO via non-covalent π - π stacking interaction and is released from GO once forming ds-DNA or G-quadruplex.³⁰ The fluorescent signal of FAM labelled on ss-DNA is then correspondingly modulated under the synergistic action of GO and DNA (See Figure S1, S3 in supporting information (SI) and discussions in the main text).

To establish optimal conditions, concentrations of GO and DNAs were explored (See Figure S2-S3 in SI). The fluorescence of FAM shows a time-dependent restore after adding the inputs. The incubation time is then found after the fluorescence signal reaching a platform (See Figure S4 in SI). All the used DNA sequences can be found in Table 1.

An XOR logic gate is required for both HA and HS functions. Thus, the discussion is firstly concentrated on the FAM-related XOR logic operation with HS function as a sample. In the absence of any input, the system keeps at its initial state. The *t*-DNA binds on GO via noncovalent π - π stacking interaction, forming GO/*t*-DNA complex. A low fluorescence of FAM is monitored due to the LrRET between GO and fluorophore, Fig. 2A (a). In the presence of either input, the *t*-DNA partially complements with HS-1 or HS-2 to form duplex of *t*-DNA/HS-1 or *t*-DNA/HS-2 and then releases from the GO. The FAM fluorophore is then far away from the GO, leading a restored high output signal, Fig. 2A (b, c).⁴¹ In the coexistence of the two inputs, DNA duplex of HS-1/HS-2 is generated since it presents higher affinity than either *t*-DNA/HS-1 or *t*-DNA/HS-2. The hybridization of HS-1 and HS-2 suppresses desorption of *t*-DNA from the GO, producing a low output signal, Fig. 2A (d). Here, the input is defined as "1" or "0" when input is presence or absence. Similar to the approach used in electronics, the output signal has an undefined range that it is defined as "1" or "0" when the normalized fluorescent intensity is higher than 0.35 or lower than 0.25. The definition is available for all the logic gates in this work. The fluorescent responses of FAM at 521 nm was plotted as column bar in Fig. 2B, producing the corresponding truth table, Fig. 2D. Obviously, the result fits the characteristic of XOR logic gate which performs the DIFFERENCE digit function of HS.

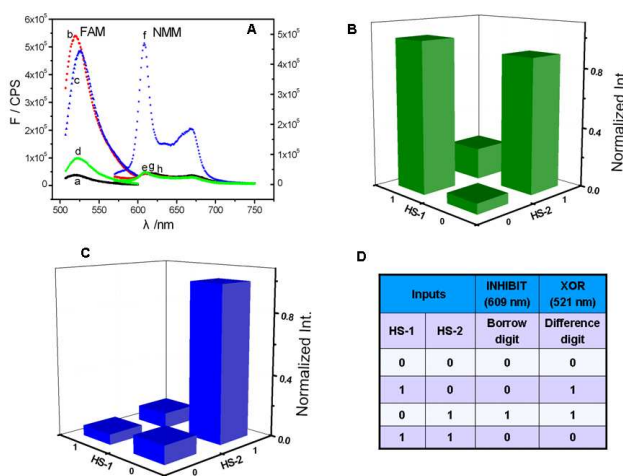


Fig. 2 (A) The output signals of FAM and NMM for the half subtractor operation triggered by the various inputs. (a, e) in the absence of the two inputs, (b, g) in the presence of HS-1 (250 nM), (c, f) in the presence of HS-2 (300 nM), (d, h) in the presence of the two inputs. The normalized fluorescence intensity of FAM at 521 nm (B) and NMM at 609 nm (C) as a function of the various inputs (HS-1 and HS-2). (D) The truth table of the HS logic operation.

All the above mentioned DNA interaction was validated by analyzing the thermal melting curves of the formed DNA duplex, Fig. 3A. The melting temperature (T_m) is 41.4°C and 49.4°C for *t*-

DNA/HS-1 and *t*-DNA/HS-2, respectively. HS-1/HS-2 shows the highest melting temperature, 74.1°C, indicating the most stability among the DNA duplexes.⁴² Native polyacrylamide gel electrophoresis (PAGE) experiments were performed to further identify the DNA interactions, Fig. 3B. From Lane 1 to Lane 3, the belts show the individual DNA of *t*-DNA, HS-1 and HS-2 in sequence. In the coexistence of any two DNAs, (HS-1 and HS-2), (*t*-DNA and HS-1) or (*t*-DNA and HS-2), new belts appear from Lane 4 to Lane 6. The results indicate the formation of duplexes of HS-1/HS-2, *t*-DNA/HS-1 and *t*-DNA/HS-2. In the coexistence of HS-1, HS-2 and *t*-DNA, one belt appears at the level of *t*-DNA, another belt appears at the level of duplex HS-1/HS-2 as shown in Lane 7. The results of PAGE, T_m measurement and fluorescence experiments are consistent with each other.

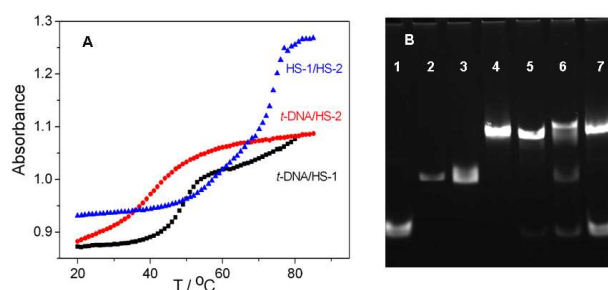


Fig. 3 (A) Thermal denaturation curves of the three DNA duplexes (100 μM), *t*-DNA/HS-1, *t*-DNA/HS-2, and HS-1/HS-2. The absorbance was monitored at 260 nm, the interval temperature is 1°C and the ramp rate is 1°C/min. (B) PAGE analysis of *t*-DNA (1), HS-1 (2), HS-2 (3), HS-1/HS-2 (4), *t*-DNA/HS-1 (5), *t*-DNA/HS-2 (6), and HS-1/HS-2 (7).

The arithmetic function of HS is realized based on the performance of XOR and INHIBIT logic gates in parallel. As the requirement, a NMM related INHIBIT logic gate was realized accompanying the XOR logic gate in the developed system. In the absence of any input, the system shows a low fluorescent output signal of NMM, Fig. 2A (e). The input HS-2 is G-riched at 3'-terminal and can form G-4 configuration (See Figure S5A in SI). NMM is then binding on G-4, producing a greatly enhanced signal, Fig. 2A (f). The input HS-1 is C-riched at 5'-terminal and cannot form G-4 configuration to enhance the NMM signal Fig. 2A (g). In the coexistence of the two inputs, the formed duplex HS-1/HS-2 inhibits the formation of G-4. A low NMM fluorescent signal is then monitored. Fig. 2C shows the column bar of NMM signal at 609 nm, producing the truth table Fig. 2D. In briefly, the output of the system is "1" only when the input HS-2 is added, fitting the feature of an INHIBIT logic operation. According to the above discussion, the developed XOR logic gate and INHIBIT logic gate can be performed in parallel triggered by the same set of input, which code for the DIFFERENCE and the BORROW digits of HS, respectively.

To fulfill the requirements of increased computational complexity, it is of importance to construct multi-component devices on a universal molecular platform.²⁰ Here, the above developed GO/DNA platform was still used to further implement HA arithmetic logic function. For HA function, an XOR logic gate is also required. Thus, a similar strategy as that in HS was utilized to design the inputs of HA with FAM as signal indicator. Either input 1 (HA-1) or input 2 (HA-2) can strip the *t*-DNA from GO by forming duplex of *t*-DNA/HA-1 or *t*-DNA/HA-2. In the

coexistence of the two inputs, duplex of HA-1/HA-2 rather than *t*-DNA/HA-1 or *t*-DNA/HA-2 is formed, leaving the *t*-DNA on the GO surface. The DNA interactions were validated by thermal melting experiments (See Figure S6 in SI). The optimal experimental conditions were explored and can be found in supporting information (See Figure S7, S8). FAM reports high outputs in the presence of each of the inputs (Fig. 4A (b, c)) and low outputs in other cases (Fig. 4A (a, d)), corresponding to the required XOR logic operation. Besides an XOR logic gate, an AND logic gate is required for a HA function. Here, a split G-4 (3:1) strategy was utilized to design the inputs with NMM as signal indicator. The HA-1 contains three guanine bases at 5'-terminal and HA-2 contains G-rich sequence (GGGTTTGGGTTTGGG) at 3'-terminal. The G-4 cannot form when the system is subjected to any of the inputs or without inputs,⁴³ producing a low output signal, Fig. 4A (e, f and g). When the two inputs are added simultaneously, G-4 is generated through hybridization of HA-1 and HA-2 (See Figure S5B in SI). NMM presents a dramatically enhanced fluorescence signal after its binding to the G-4, Fig. 4A (h). The normalized fluorescence responses of FAM (521 nm) and NMM (609 nm) were plotted as column bar in Fig. 4B and Fig. 4C, respectively, producing the corresponding truth table, Fig. 4D. According to the above discussion, the XOR and the AND logic gates were realized in parallel on the universal platform triggered by the same set of inputs and coded for SUM and CARRY digits, respectively. The results fulfill the requirements of HA logic function.

The DNA logic gates are important components of DNA computing and have been demonstrated its application in biomedical field for disease diagnosis and therapy due to its biocompatibility.² The logic operations demonstrated here also present potential application in disease diagnosis. For example, if two disease-related markers are used as inputs, the AND gate of the HA can perform function to present TRUE signal, indicating coexistence of the two markers. The XOR gate can perform function to present TRUE signal, indicating the existence of each marker. While, for potential application in disease diagnosis, one

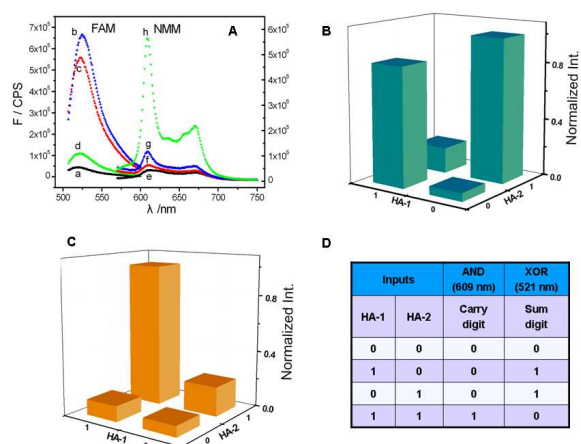


Fig.4 (A) The output signals of FAM and NMM for the half adder operation triggered by the various inputs. (a, e) in the absence of the two inputs, (b, f) in the presence of HA-1 (250 nM), (c, g) in the presence of HA-2 (250 nM), (d, h) in the presence of the two inputs. The normalized fluorescence intensity of FAM at 521 nm (B) and NMM at 609 nm (C) as a function of the various inputs. (D) The truth table of the HA logic operation.

has to consider photo bleaching and high background of the used fluorophore. Upconversion fluorescence nanoparticles (UCNPs) can convert two or more near-infrared-light pump photons into a higher energy output photon, greatly reducing background interference.⁴⁴ Additionally, UCNPs presents exceptional photo stability, high quantum yields and long lifetime and has been considered as an excellent candidate in disease diagnosis.⁴⁵

In the present investigations, arithmetic functions of HA and HS have been successfully realized on a simple and universal GO/*t*-DNA platform for the first time. The operation is simple and convenient and is realized in an enzyme-free condition by taking advantage of GO and DNA. Here, GO works as an effective fluorophore quencher and also as substrate to trap ss-DNA while neither ds-DNA nor G-4. Combining the versatile configuration variations of DNA such as single strand, duplex and G-4, the fluorescent signal of the system can be flexibly modulated under stimulation of the inputs. The synergistic functions of GO and DNA strands can simplify the design and performance of arithmetic function. The developed system overcomes the limitations that the required logic gates are implemented on different platform or triggered by different inputs. Here, the required logic gates of HS respond to the same set of inputs, which is the same case for the HA logic operation. All required logic operations by both HA and HS were realized on a universal platform. A constant undefined output range between high and low output signals was set and available for all the required logic operations. The investigation provides a simple and convenient way for integration of multiple logic circuits on a universal platform to implement arithmetic functions. The advantages make it possible for potential application of the developed logic gate in DNA computing and disease diagnosis.

This work was supported by the National Natural Science Foundation of China (Nos. 21105095 and 211900040), State Key Instrument Developing Special Project of Ministry of Science and Technology of China (2012YQ170003), the Instrument Developing Project of the Chinese Academy of Sciences (YZ201203) and the Natural Science Foundation of Jilin Province, China (No. 20130101117JC).

Notes and references

- ^a State Key Laboratory of Electroanalytical Chemistry, Changchun Institute of Applied Chemistry, Chinese Academy of Sciences, Changchun 130022, and University of Chinese Academy of Sciences, Beijing, 100039, China
Corresponding Authors: yaqingliu@ciac.ac.cn; ekwang@ciac.ac.cn.
 - ^b Department of Chemistry and Environmental Engineering, Changchun University of Science and Technology, Changchun, China.
- † Electronic Supplementary Information (ESI) available: [details of any supplementary information available should be included here]. See DOI: 10.1039/b000000x/
- L. M. Adleman, *Science*, 1994, **266**, 1021-1023.
 - Z. Xie, L. Wroblewska, L. Prochazka, R. Weiss and Y. Benenson, *Science*, 2011, **333**, 1307-1311.
 - M. N. Stojanovic, T. E. Mitchell and D. Stefanovic, *J. Am. Chem. Soc.*, 2002, **124**, 3555-3561.
 - F. Xia, X. Zuo, R. Yang, R. J. White, Y. Xiao, D. Kang, X. Gong, A. A. Lubin, A. Vallée-Bélisle and J. D. Yuen, *J. Am. Chem. Soc.*, 2010, **132**, 8557-8559.
 - T. Gupta and M. E. van der Boom, *Angew. Chem., Int. Ed.*, 2008, **47**, 5322-5326.

6. S. Erbas-Cakmak and E. U. Akkaya, *Angew. Chem., Int. Ed.*, 2013, **52**, 11364-11368.
7. A. Coskun, E. Deniz and E. U. Akkaya, *Org. Lett.*, 2005, **7**, 5187-5189.
8. A. P. de Silva and S. Uchiyama, *Nat. Nanotechnol.*, 2007, **2**, 399-410.
9. A. J. Genot, J. Bath and A. J. Turberfield, *J. Am. Chem. Soc.*, 2011, **133**, 20080-20083.
10. D. Han, Z. Zhu, C. Wu, L. Peng, L. Zhou, B. Gulbakan, G. Zhu, K. R. Williams and W. Tan, *J. Am. Chem. Soc.*, 2012, **134**, 20797-20804.
11. H. Li, W. Hong, S. Dong, Y. Liu and E. Wang, *ACS Nano*, 2014, **8**, 2796-2803.
12. B. Shlyahovsky, Y. Li, O. Lioubashevski, J. Elbaz and I. Willner, *ACS nano*, 2009, **3**, 1831-1843.
13. W. Hong, Y. Du, T. Wang, J. Liu, Y. Liu, J. Wang and E. Wang, *Chem.-Eur. J.*, 2012, **18**, 14939-14942.
14. B. Gulbakan, E. Yasun, M. I. Shukoor, Z. Zhu, M. You, X. Tan, H. Sanchez, D. H. Powell, H. Dai and W. Tan, *J. Am. Chem. Soc.*, 2010, **132**, 17408-17410.
15. Y. Liu, J. Ren, Y. Qin, J. Li, J. Liu and E. Wang, *Chem. Commun.*, 2012, **48**, 802-804.
16. K. S. Park, M. W. Seo, C. Jung, J. Y. Lee and H. G. Park, *small*, 2012, **8**, 2203-2212.
17. J. Elbaz, O. Lioubashevski, F. Wang, F. Remacle, R. D. Levine and I. Willner, *Nat. Nanotechnol.*, 2010, **5**, 417-422.
18. H. Pei, L. Liang, G. Yao, J. Li, Q. Huang and C. Fan, *Angew. Chem.*, 2012, **124**, 9154-9158.
19. D. Miyoshi, M. Inoue and N. Sugimoto, *Angew. Chem., Int. Ed.*, 2006, **45**, 7716-7719.
20. D. Kang, R. J. White, F. Xia, X. Zuo, A. Vallée-Bélisle and K. W. Plaxco, *NPG Asia Materials*, 2012, **4**, e1.
21. S. Bi, B. Ji, Z. Zhang and J.-J. Zhu, *Chem. Sci.*, 2013, **4**, 1858.
22. C. M. Niemeyer, *Angew. Chem., Int. Ed.*, 2001, **40**, 4128-4158.
23. T. Li, L. Zhang, J. Ai, S. Dong and E. Wang, *ACS nano*, 2011, **5**, 6334-6338.
24. M. Pita, M. Krämer, J. Zhou, A. Poghossian, M. J. Schöning, V. c. M. Fernández and E. Katz, *ACS nano*, 2008, **2**, 2160-2166.
25. D. Chen, L. Tang and J. Li, *Chem. Soc. Rev.*, 2010, **39**, 3157-3180.
26. C.-N. Yang, C.-Y. Hsu and Y.-C. Chuang, *Chem. Commun.*, 2012, **48**, 112-114.
27. X. Liu, R. Aizen, R. Freeman, O. Yehezkeili and I. Willner, *ACS nano*, 2012, **6**, 3553-3563.
28. R. Swathi and K. Sebastian, *J. Chem. Phys.*, 2008, **129**, 054703.
29. W. Y. Xie, W. T. Huang, N. B. Li and H. Q. Luo, *Chem. Commun.*, 2012, **48**, 82-84.
30. L. Wang, J. Zhu, L. Han, L. Jin, C. Zhu, E. Wang and S. Dong, *ACS nano*, 2012, **6**, 6659-6666.
31. Y. He and H. Cui, *Chem.-Eur. J.*, 2013, **19**, 13584-13589.
32. Y. Lin, Y. Tao, F. Pu, J. Ren and X. Qu, *Adv. Func. Mater.*, 2011, **21**, 4565-4572.
33. L. Tang, D. Li and J. Li, *Chem. Commun.*, 2013, **49**, 9971-9973.
34. A. Okamoto, K. Tanaka and I. Saito, *J. Am. Chem. Soc.*, 2004, **126**, 9458-9463.
35. S. Xu, H. Li, Y. Miao, Y. Liu and E. Wang, *NPG Asia Mater.*, 2013, **5**, e76.
36. R. Orbach, F. Wang, O. Lioubashevsky, R. Levine, F. Remacle and I. Willner, *Chem. Sci.*, 2014.
37. H. Li, J. Ren, Y. Liu and E. Wang, *Chem. Commun.*, 2014, **50**, 704-706.
38. H. Li, J. Liu, Y. Fang, Y. Qin, S. Xu, Y. Liu and E. Wang, *Biosens. Bioelectron.*, 2013, **41**, 563-568.
39. R. Swathi and K. Sebastian, *J. Chem. Phys.*, 2009, **130**, 086101.
40. W. Wu, H. Hu, F. Li, L. Wang, J. Gao, J. Lu and C. Fan, *Chem. Commun.*, 2011, **47**, 1201-1203.
41. C.-H. Lu, H.-H. Yang, C.-L. Zhu, X. Chen and G.-N. Chen, *Angew. Chem., Int. Ed.*, 2009, **48**, 4785-4787.
42. R. M. Wartell and A. S. Benight, *Physics Reports*, 1985, **126**, 67-107.
43. D. M. Kolpashchikov, *Chem. Rev.*, 2010, **110**, 4709-4723.
44. J. Zhou, Z. Liu, F. Li, *Chem. Soc. Rev.* 2012, **41**, 1323-1349.
45. Y. Yang, Q. Zhao, W. Feng, F. Li, *Chem. Rev.* 2013, **113**, 192-270.